Building Tomorrow's Society
Bâtir la Société de Demain

Fredericton, Canada
June 13 – June 16, 2018/ *Juin 13 – Juin 16, 2018*

LABORATORY MEASUREMENTS OF NEAR-BED FLOW VELOCITY OVER ROUGHNESS ELEMENTS IN AN OPEN CHANNEL

Li, Jing[1] and Li, S. Samuel[2,3]
[1] Graduate Student, Dept. of Building, Civil and Environmental Engineering, Concordia Univ., 1455 de Maisonneuve Blvd. W., Montreal, QC, Canada H3G 1M8
[2] Professor, Dept. of Building, Civil and Environmental Engineering, Concordia Univ., 1455 de Maisonneuve Blvd. W., Montreal, QC, Canada H3G 1M8
[3] (Corresponding author) E-mail: sam.lil@concordia.ca

Abstract: Roughness elements at the channel-bed have a significant influence on the characteristics of near-bed flow. To create roughness in laboratory channels, earlier researchers have used rectangular ribs and irregular gravel. Elements in the form of square-shaped cubes are arguably more suitable to quantify the influence. Experiments for detailed velocity measurements over cubes are rare. This paper reports flume experiments of flow over acrylic cubes, and investigates the flow characteristics. The flow depth ranges from 8.8 to 9.1 cm. Cubes with sides of 1.905 cm are uniformly mounted at a horizontal bed. The experiments covers three conditions of cube-crest to crest spacing: being 2, 4, and 6 times the cube side dimensions. These relative spacing conditions represent d-type, intermedium type, and k-type roughness, respectively. Flow velocities at locations above and around the cubes are measured using an ADV. At each location, the measurements last 60 s, at a sampling frequency of 120 Hz. The position of the ADV probe is controlled by a step motor, which could allow a moving distance of as small as 1 mm. In the horizontal, the measuring section extends from the upstream edge of the cube of interest to the downstream edge of the next downstream cube. In the vertical, the measurements nearest to the bed are 2 mm above it. This paper discusses velocity and shear stress distributions. The results show distinct vertical profiles of mean flow velocities and turbulence parameters under different roughness types.

1 Introduction

Turbulent flows in open channels have many important applications (Soulsby, 1983; Gross et al., 1994; Coleman et al., 2007). Previously, researchers have extensively studied velocity and bed shear stress distributions of open-channel flows. Mostly, they made measurements above a smooth channel-bed, irregular gravel bed, or bed with vegetation (Flack et al., 2007; Nikora and Goring, 2000; Wang et al., 2012; Wang et al., 2015; Yurtal, 2006). Few experimental studies dealt with uniformly distributed roughness of regular shape. Some used rectangular ribs to create bed roughness. For example, Coleman et al. (2007) measured vertical profiles of velocity over two consecutive ribs. Detailed flow structures in the along- and cross-channel directions around roughness elements are also important, but have not received adequate attention. This paper aims to measure 3-D turbulent flow over cubes (Figure 1).

Let L denote the cube spacing, and h denote the roughness height (Figure 1). Perry et al. (1969) categorised roughness types as d-type, intermediate type and k-type. The d-type has the smallest L/h ratio, the k-type has the largest L/h ratio, and the intermediate type is in between. According to Simpson (1973) and Jiménez (2004), the roughness type is d-type when $L/h < 4$, k-type when $L/h > 5$. This paper covers roughness conditions of $L/h = 2$ (d-type), 4 (intermediate type), and 6 (k-type).

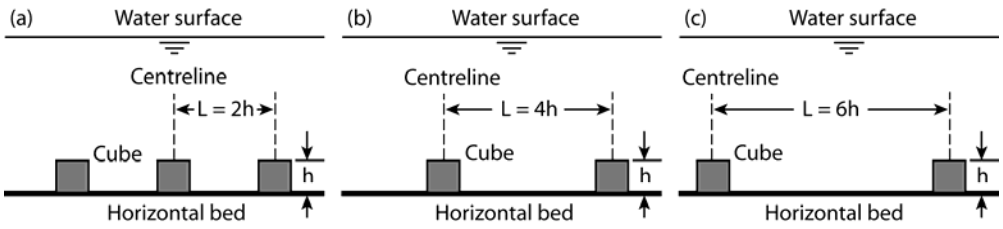

Figure 1: Cubes as roughness elements; roughness types are: a) d-type; b) intermediate type; c) k-type.

Different methods for estimating bed shear stress have been reported in the literature. Biron et al. (2004) provided assessments of four methods: gravity method, logarithmic profile (LP) method, turbulence kinetic energy (TKE) (and TKE-ω) method, and Reynolds shear stress (RSS) method. According to them, under smooth bed condition, the gravity method produces the highest estimates of bed shear stress among the four methods. The RSS and TKE methods give similar estimates. They suggested that the TKE method is the most accurate method for complex flow. Some researchers compared the different methods for marine and estuary applications. For instance, using the LP, RSS, TKE, and ID methods, Ali and Lemckert (2009) calculated bed shear stress in Coombabah Creek, Australia. They suggested that the LP method was the most reliable. Inoue et al. (2011) made similar comparisons. On the one hand, the earlier studies did not deal with uniformly distributed cubes. On the other hand, uncertainties exist about whether or not the measurements used in the studies include data from positions close enough to the bed. The remaining part of this paper gives a description of the experimental setup for velocity measurements, followed by data processing. Next, the experimental results are discussed before conclusions are drawn.

2 Experimental Methods

2.1 Experimental Setup

Experiments of flow over an array of cubes (Figure 1) were carried out in the Water Resources Laboratory at Concordia University. The setup consists of a flume channel of rectangular shape, water supply reservoir, pump, and electromagnetic flowmeter (Figure 2). The channel has vertical tempered-glass sidewalls and a flat stainless steel bed with zero slope. Acrylic cubes arranged in rows and columns were mounted at the bed (Figure 1). The channel has an inlet section attached to its upstream end and an outlet section to its downstream end. Pipes connect the reservoir, inlet section, flume, and outlet section.

During an experiment, water from the reservoir flows through the inlet section, channel, outlet section and returns to the reservoir. The inlet section has curved sidewalls that cause streamlines to contract in the horizontal plane, and thus help create uniform approach flow to the channel. This section has a plate that floats at the water surface for damping turbulence in the approach flow. The outlet section has an adjustable tail gate for the control of flow depth in the channel.

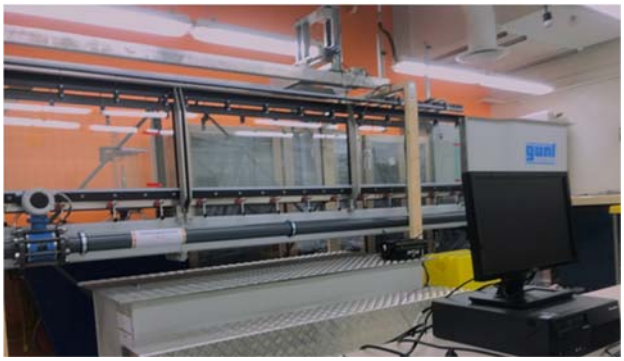

Figure 2: Experimental setup, showing a flume channel, an inlet section attached to its upstream end, and a step motor rig supported by a pair of railings over the top of the channel.

The channel (Figure 2) is 500 cm long, and 30 cm wide. The cubes have a roughness height of 1.905 cm (or 3/4 inches). For d-type roughness (L/h = 2, Figure 1), a total of 336 cubes were mounted at a flat acrylic plate of 182.9 cm long and 29.2 cm wide; for the intermediate type (L/h = 4), a total of 72 cubes were mounted; for the k-type (L/h = 6), a total of 48 cubes were mounted. The plate with cubes mounted was placed at the bed; its upstream edge was located at a distance of 2 m downstream of the channel entrance. The upstream edge of the plate is a ramp that causes vertical contraction of streamlines. This helps create uniform flow before entering the channel section for velocity measurements. The distance of 2 m ensures that the flow is fully developed at the channel section for measurements. The criterion is that the distance is larger than the entrance length, L_e, (Table 1) for fully developed flow, which is given by $L_e = 4.4\mathrm{Re}^{1/5}D$, where Re is the Reynolds number; D is the hydraulic radius.

Table 1: Conditions of flume experiments of flow over cubes

Experiment	Cube spacing to height ratio L/h	Discharge Q (L/s)	Flow depth H (cm)	Re*	Entrance length L_e (m)
1	2	14.72	8.8	29095	1.42
2	4	14.76	9.0	28932	1.41
3	6	14.46	9.0	28344	1.40

The discharge was measured using an electromagnetic flowmeter. The flow depth is about 9 cm above the plate surface. During an experiment, the pump delivers water from the reservoir. Water enters the channel, reaches the upstream edge of the plate, submerges the cubes, and passes through the entire channel. Then, the water enters the outlet section, where adjustment of the tail gate controls the flow depth. Next, the water exits the outlet section and returns to the reservoir.

2.2 Data Collection

ADV measurements of 3-D flow velocities above and around cubes were made. The ADV probe was mounted on a rig and its positioning was achieved accurately by using the step motor (Figure 2). As for the ADV configurations, the key parameters are: The sampling volume is 2.8 mm; the velocity range is ±0.3 m/s; the transmit length is 0.6 mm. The sampling volume is at a distance of 5 cm to the ADV probe.

The target regions of measurements for the three experiments (Table 1) are plotted in Figure 3. Each region is covered with a large number of locations in the horizontal. At each of these locations, velocities were measured at six elevations above the bed. The vertical distance between adjacent elevations is around 5 mm. At each elevation, the region is symmetrical about its longitudinal centreline. In the longitudinal direction, measurements were made from the upstream edge of the first cube to the downstream edge of the third cube. In the along-channel direction (or the x-direction), the spacing between two adjacent measurement locations at the same elevation is 5.7 cm. In the cross-channel direction (or the y-direction), the spacing is 4.5 mm. At each location, the duration of measurement is one minute, which yields the same statistics as 3-minute measurements. The measurement locations are listed in Table 2, and are illustrated in Figure 4 as an example.

Table 2: Vertical elevation Z of measurements and the total number of measurement points, N, at each elevation. The measurements nearest to the bed is from a vertical distance of 2 mm above it.

Experiment	N	Z (cm)					
1	143	0.2	0.7	1.5	2.0	2.5	3.1
2	306	0.2	0.7	1.4	1.9	2.5	3.0
3	792	0.2	0.7	1.5	1.9	2.5	3.1

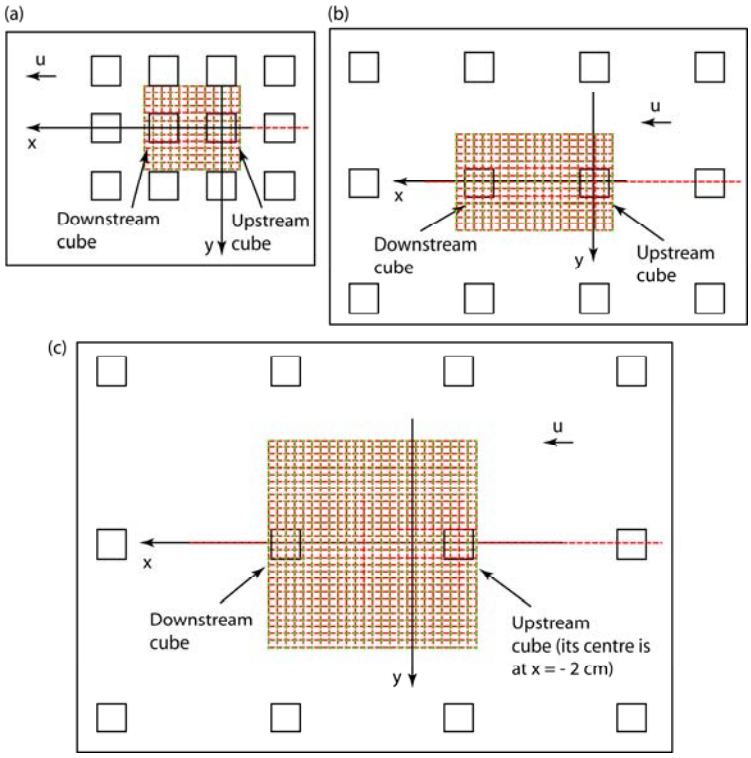

Figure 3: Top view of the target regions (the red grids) for velocity measurements: (a) L/h = 2; (b) L/h = 4; (c) L/h = 6. The green dots show the measurement locations in the horizontal. The open squares are the cubes of 1.905 cm in side dimensions. The total number of cubes mounted at the bed is 336, 72 and 48 for the cases of L/h = 2, 4, and 6, respectively.

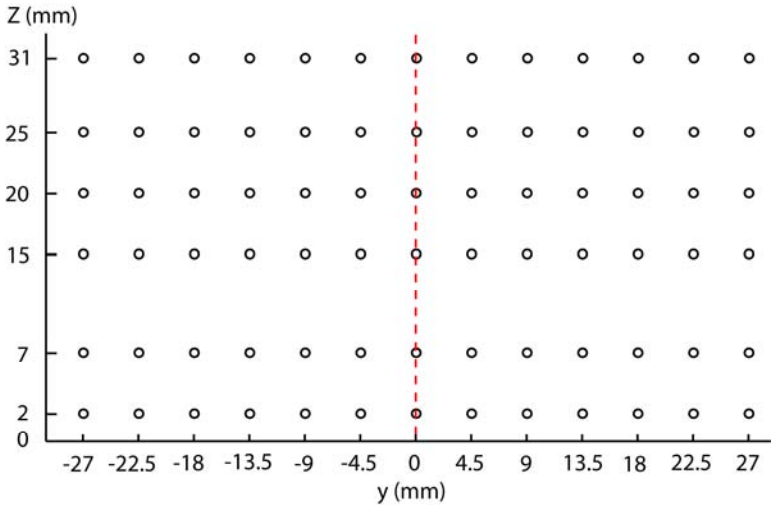

Figure 4: A vertical plane showing measurement locations (circles).

3 Preliminary Results

The raw ADV data was filtered using the Velocity Signal Analyser ("VSA", v.1.5.62), following the process given in Jesson et al. (2015). This involves setting Phase-Space Thresholding in order to de-spike and filter the raw data. Then, the filtered velocities were processed and analysed using MATLAB code. Distinct velocity profiles have been identified.

Examples of vertical profiles of the longitudinal velocity *u* for *L*/*h* = 6 are discussed below. The channel-bed is located at Z = 0. The profiles are plotted in Figures 5 and 6 for *x* = 20 mm, at locations across the channel through the first cube [the upstream cube, Figure 3(c)]. The profiles are shown in Figures 7 and 8 for x = -5, at about 23 cm away from the downstream edge of the first cube [the upstream cube, Figure 3(c)].

Clearly, *u* increases with *Z* and reaches a maximum value at *Z* = 30 mm. The minimum value of *u* occurs nearest to the bed. The velocity data from *Z* = 30, 25, 20 and 15 (or 14) mm appear to follow typical boundary layer distributions, whereas the velocity data from *Z* = 2 and 7 mm have different patterns. In some cases, *u* changes rapidly between *Z* = 2 mm and *Z* = 7 mm, and even between *Z* = 7 and *Z* = 14 mm. This is case at coordinates (20, 32) in Figure 5, at coordinates (-5, 32) in Figure 7, and at coordinates (-5, -36) in Figure 8.

One can see two distinct types of profiles for *L*/*h* = 6. The first type of these appears to have linear distribution between the bed and water surface. An example is given at the coordinates (-5, -20) in Figure 8. In this case, u is usually larger at Z =14 mm than at Z = 7 mm. The second type of profiles features a sudden change of u at the second lowest elevation (Z = 7 mm). This is the case at coordinates (20, 40) and coordinates (20, 32) in Figure 5. In this case, u is larger at Z = 7 mm than Z =14 mm. Further up in the water column, u seems to increase linearly toward the water surface. For L/h = 4 and L/h = 2, the types of velocity profiles are similar to those for L/ h =6. It should be noticed that for L/h = 4, more profiles belong to the first type of profiles than for L/ h = 6.

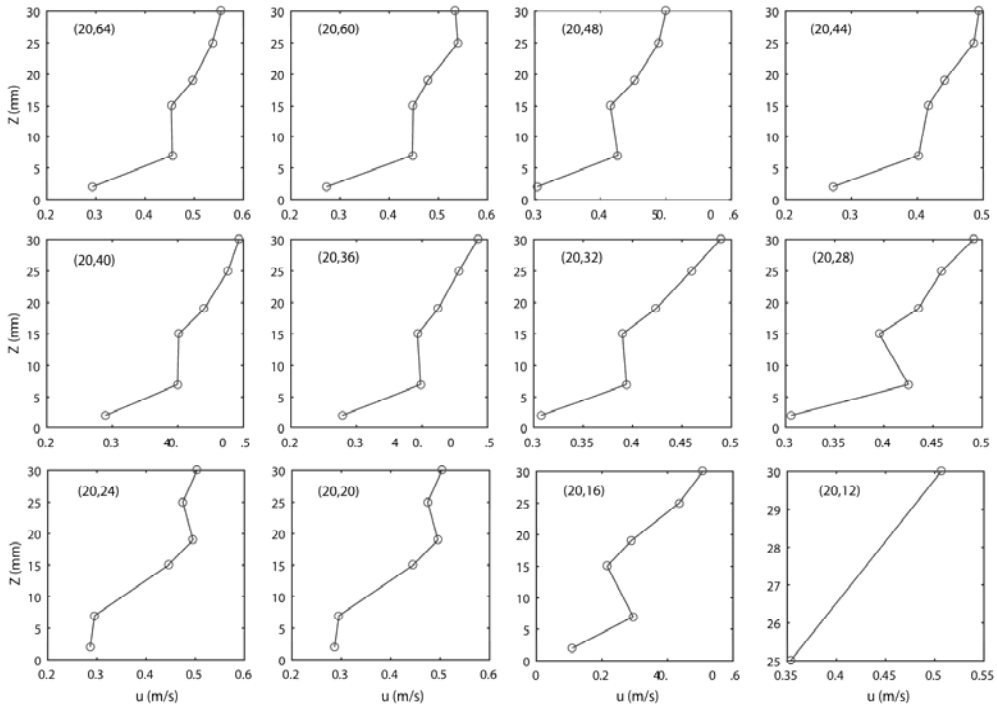

Figure 5: Vertical profiles of the longitudinal velocity *u* at x = 20 (to the right of the central cubes). For the 12 panels, the y-coordinates are 64, 60, 48, 44, 40, 36, 32, 28, 24, 20, 16, and 12, respectively.

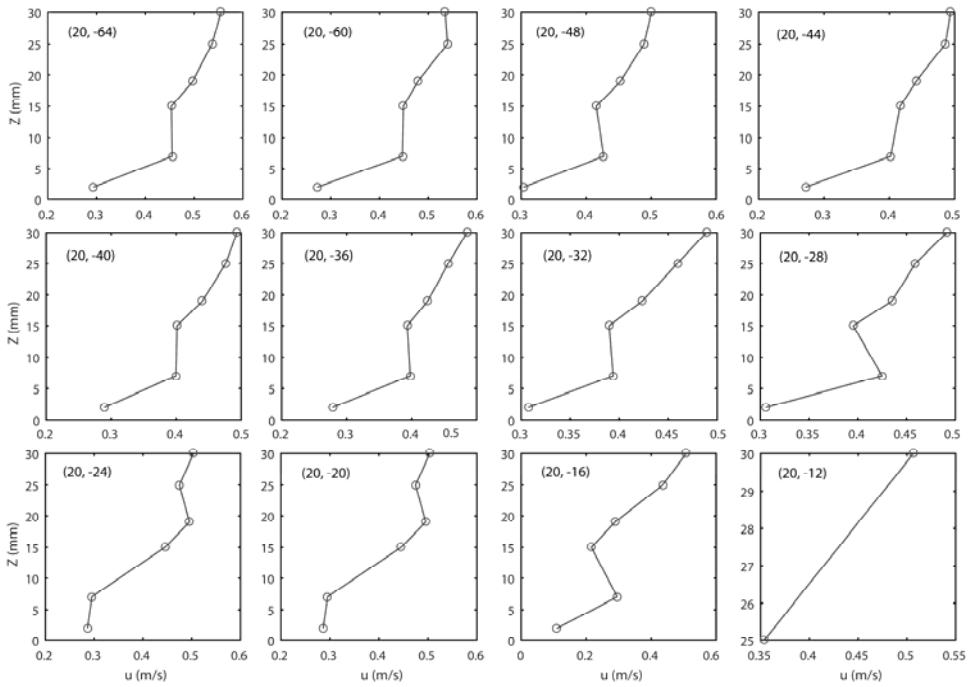

Figure 6: Vertical profiles of the longitudinal velocity u at x = 20 (to the left of the central cubes). For the 12 panels, the y-coordinates are -64, -60, -48, -44, -40, -36, -32, -28, -24, -20, -16, and -12, respectively.

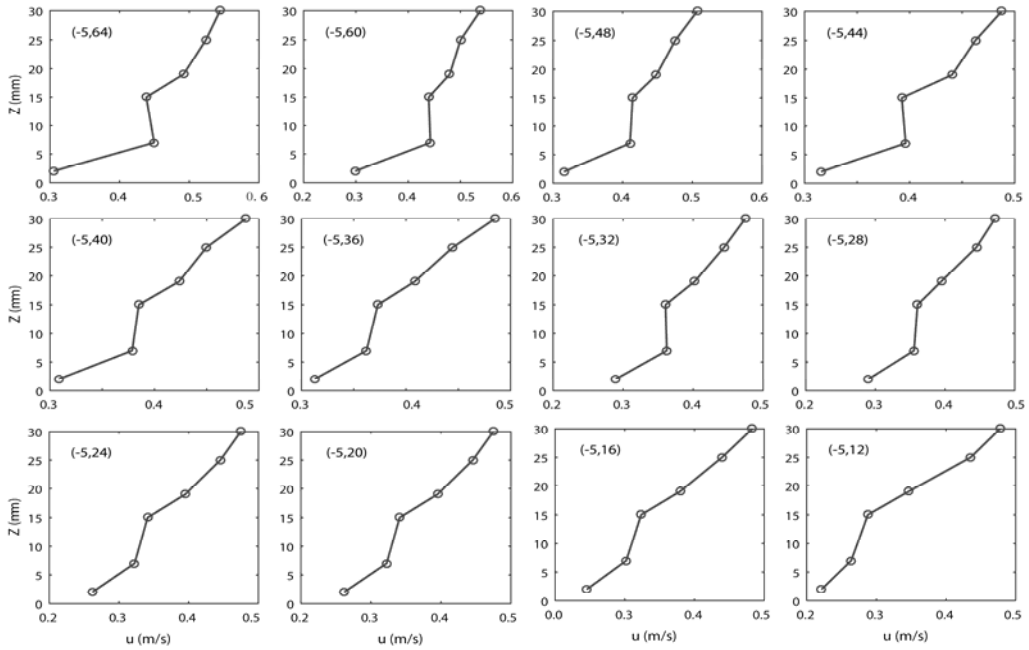

Figure 7: Vertical profiles of the longitudinal velocity u at x = -5 (to the right of the central cubes)

An examination of u contour distributions (not shown) displays slightly asymmetrical patterns about the centreline of the symmetrical target region. This is based on the distributions at Z = 25 mm (9 mm above the top surface of cubes). Water circulates to the downstream face of cubes around the lateral faces, meaning that an exchange of momentum in the across-channel direction. It would be interesting to carry out further analysis on the basis of momentum principle and determine the forces exerted by the flowing

water on the cubes. Such information will be used for sediment transport application. In addition, further analysis of turbulence parameters is of importance.

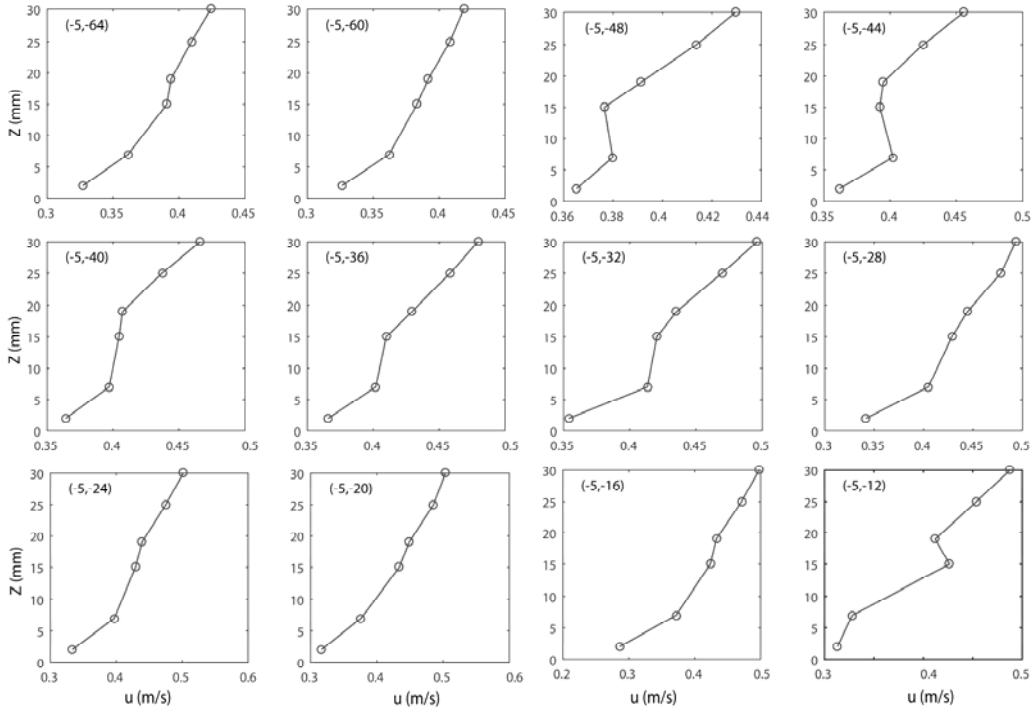

Figure 8: Vertical profiles of the longitudinal velocity u at x = -5 (to the left of the central cubes)

We used the filtered data to calculate the Reynolds shear (RS) stress for each measurement point. We categorized the vertical RS profiles into 11 types (Types I - XI). Types I to VI are shown in Figure 9, and types VII to XI are shown in Figure 10. Each type includes two sub-types except Type XI. The y-axis is the vertical distance from the channel-bed (Z in mm), and the x-axis is the Reynolds shear stress (RS in N/m^2).

As illustrated in Figure 10, only two types, Type X: C-L at (-55, -64) and Type VII: A-L at (-30, 52), show that RS increases uniformly with Z, and the maximum RS can be found at Z = 30 mm. Other types (e.g. Type X: CS-L) indicate an irregular change on RS: the RS increases from the channel-bed to the third point at Z = 15 mm, then changes the trend, decreases from the fourth point to the highest point at Z = 30 mm. Some types (e.g. Type IX: B-L1) illustrate a decreasing trend of RS at the three points nearer to the channel-bed, then RS suddenly increases from the 4^{th} to 5^{th} points, and decreases at Z = 30 mm. We can also find that the increasing and decreasing trends mainly present in three typical patterns: line-line pattern (Type XI: CS-L1 in Figure 10), curve-curve pattern (Type III: BS-V in Figure 9) and line-curve or curve-line combination (Type VIII: BS-L in Figure 10; Type II: AS-V1, in Figure 9).

Based on the results discussed above, we back-calculated the longitudinal velocity (u), by using the following analytical equations

[2] $\tau = \rho u_*^2$

[3] $u/u_* = 2.5 \ln (y/\kappa) + 8.5$

where τ is the bed shear stress, taken as equals to the Reynolds shear stress that we have measured; u is the longitudinal velocity component; ρ is the density of water, taken as 1000 kg/ m^2; u_* is the shear velocity; y is the vertical distance from the channel-bed; κ is Von Karman constant, taken as 0.4. The back-calculated u and measured u for each Reynolds shear stress type are plotted in Figures 11 and 12.

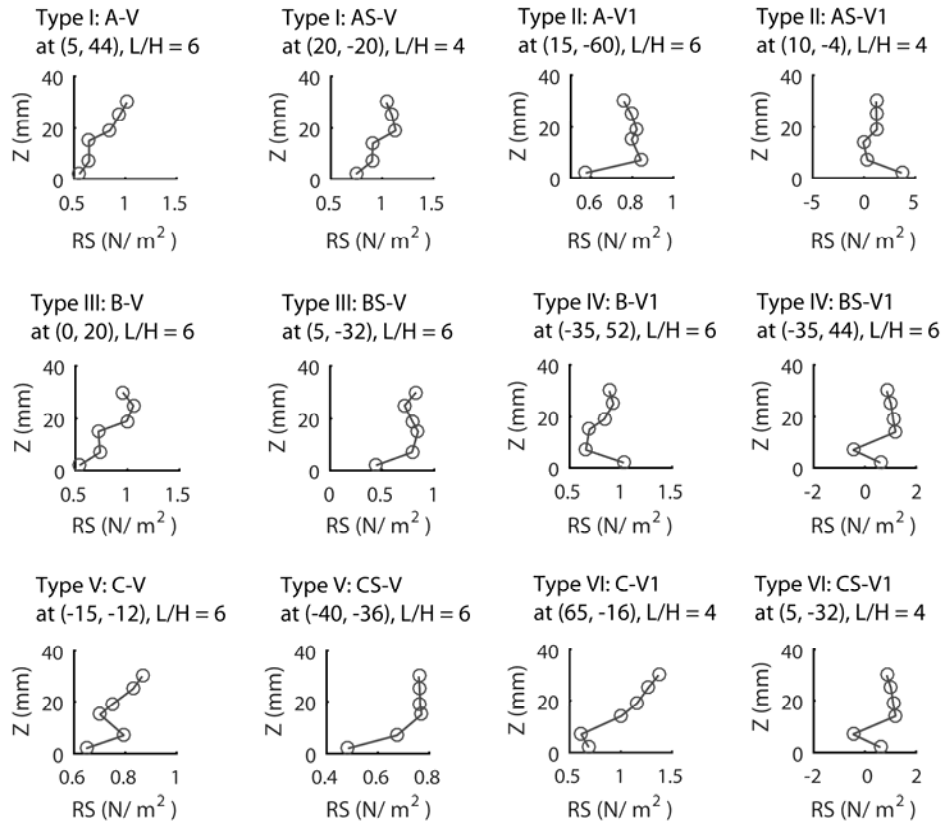

Figure 9: Vertical profiles of the Reynolds shear stress (RS): Types I to VI.

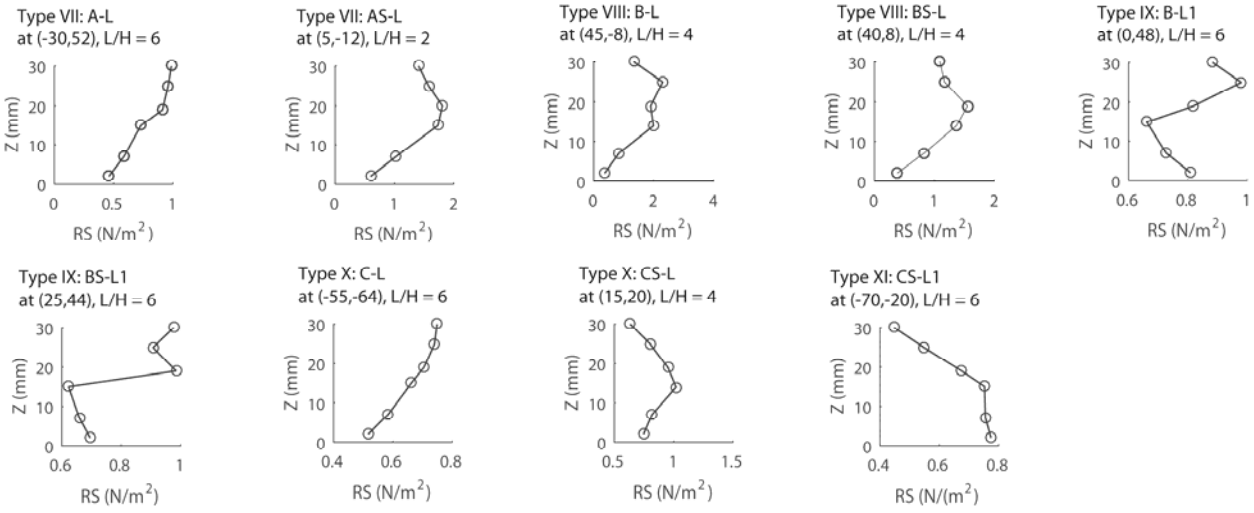

Figure 10: Vertical profiles of the Reynolds shear stress (RS): Types VII to XI

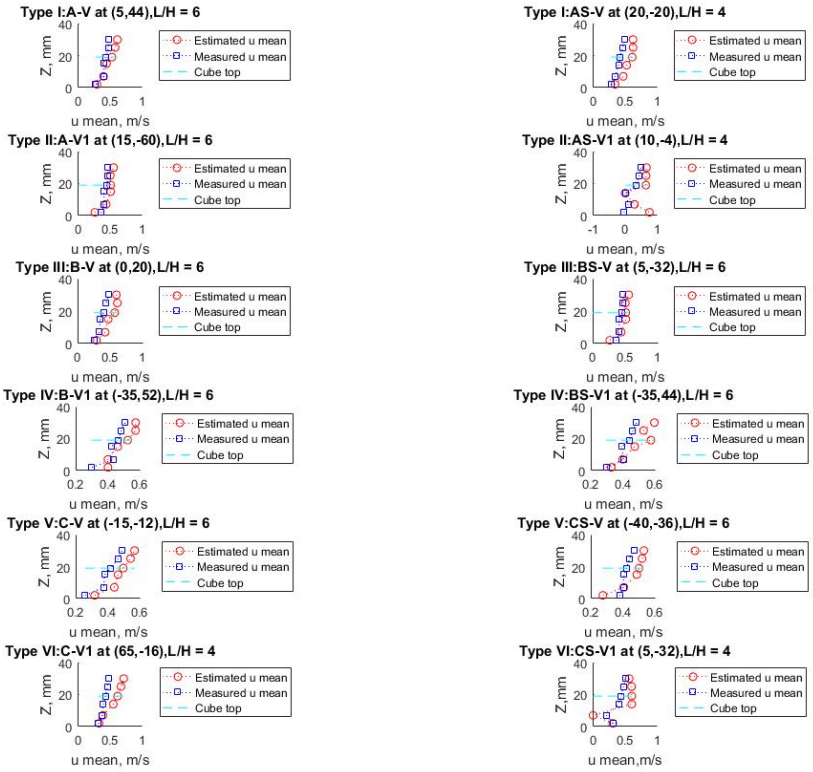

Figure 11: Comparison of back-calculated and measured u of Reynolds shear stress: Types I to VI.

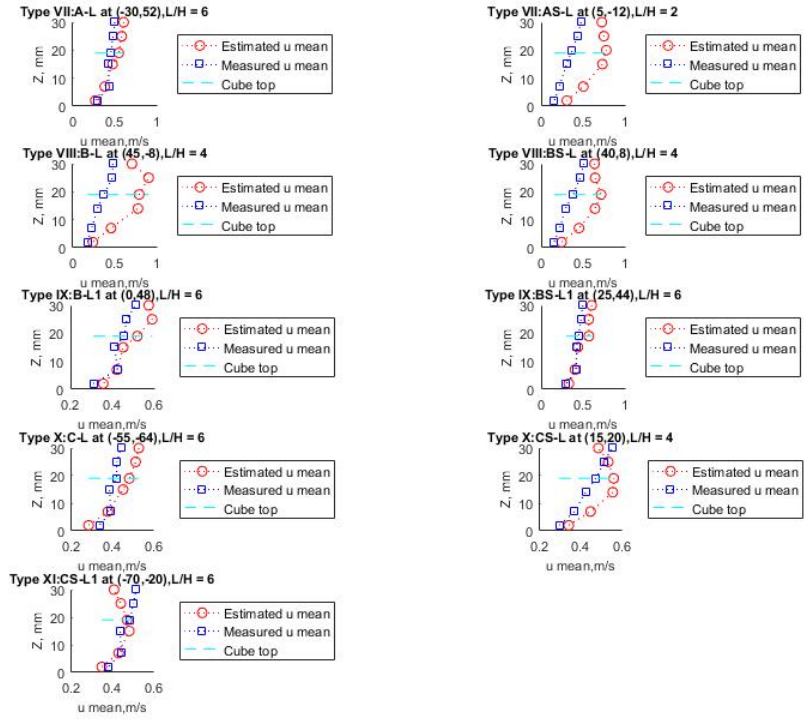

Figure 12: Comparison of back-calculated and measured u of Reynolds shear stress: Types VII to XI.

We can easily see from Figure 10 that even for the two types, Type X: C-L at (-55, -64) and Type VII: A-L at (-30, 52), in which Reynolds shear stresses are uniformly distributed better than the other types, the back-calculated u profiles do not match the measured u profiles very well. This indicates that equation [3] is inadequate to describe the vertical distribution of u in the near-bed region, and the Reynolds shear stress are not distributed uniformly.

4 Conclusions

This paper reports laboratory measurements of 3-D flow velocities over cubes as roughness elements at the channel-bed. The focus of this paper is on near-bed flow. The spacing of the roughness elements represents d-type roughness, k-type roughness and intermediate type. The velocity distributions are slightly asymmetrical about the channel centreline even though the roughness elements are strictly symmetrical. This paper contributes to the creation of a large amount of the 3-D measurements at accurate positions in the near-bed region. The experimental data leads to the identification of distinct vertical profiles of longitudinal velocity from the near-bed region. Further analysis of the data includes turbulent characteristics such as the shear velocity and Reynolds shear stress. Assessment of various methods for estimates of the turbulence parameters is discussed.

Acknowledgements

This study received financial support from NSERC through Discovery Grants held by S. Li. The authors thank the technicians Jamie Yeargans, Andy Shin-Pong and Nicolas Silva-Gastellon for their help in the Water Resources Laboratory.

References

Ali, A. and Lemckert, C.J., 2009. A Traversing System to Measure Bottom Boundary Layer Hydraulic Properties. *Estuarine, Coastal and Shelf Science*, **83**(4): 425-433.

Biron, P.M., Robson, C., Lapointe, M.F. and Gaskin, S.J., 2004. Comparing Different Methods of Bed Shear Stress Estimates in Simple and Complex Flow Fields. *Earth Surface Processes and Landforms*, **29**(11): 1403-1415.

Coleman, S.E., Nikora, V.I., McLean, S.R. and Schlicke, E., 2007. Spatially Averaged Turbulent Flow over Square Ribs. *Journal of Engineering Mechanics*, **133**(2): 194-204.

Flack, K.A., Schultz, M.P. and Connelly, J.S., 2007. Examination of a Critical Roughness Height for Outer Layer Similarity. *Physics of Fluids*, **19**(9): p.095104.

Gross, T.F., Williams, A.J. and Terray, E.A., 1994. Bottom Boundary Layer Spectral Dissipation Estimates in the Presence of Wave Motions. *Continental Shelf Research*, **14**(10-11): 1239-1256.

Inoue, T., Glud, R.N., Stahl, H. and Hume, A., 2011. Comparison of Three Different Methods for Assessing in Situ Friction Velocity: A Case Study from Loch Etive, Scotland. *Limnology and Oceanography*: *Methods* **9**(6): 275-287.

Soulsby, R.L., 1983. The Bottom Boundary Layer of Shelf Seas. *Elsevier Oceanography Series*, **35**: 189-266.

Wang, X.Y., Yang, Q.Y., Lu, W.Z. and Wang, X.K., 2012. Experimental Study of Near-Wall Turbulent Characteristics in an Open-Channel with Gravel Bed Using an Acoustic Doppler Velocimeter. *Experiments in Fluids*, **52**(1): 85-94.

Wang, X.K., Ye, C., Wang, B.J. and Yan, X.F., 2015. Experimental Study on Velocity Profiles with Different Roughness Elements in a Flume. *Acta Geophysica*, **63**(6): 1685-1705.

Yurtal, R., 2006. Shear Stress Distributions along the Cross Section in Smooth and Rough Open Channel Flows. *Kuwait Journal of Science* & *Engineering*, **33**(1):155-168.